Journal of King Saud University - Science 36 (2024) 103398

HOSTED BY

Contents lists available at ScienceDirect

Journal of King Saud University - Science

journal homepage: www.sciencedirect.com

Synthesis, characterization and density functional theory of ^{64}Cu based complex for hypoxia imaging

N. Alhokbany [a,*], I. Aljammaz [b], B. Alotaibi [b], Y. AlMalki [b], S. Almasaari [b]

[a] King Saud University, Chemistry Department, Riyadh, Saudi Arabia
[b] King Faisal Specialist Hospital & Research Centre, Riyadh, Saudi Arabia

ARTICLE INFO

Keywords:
Tumor hypoxia
Hypoxia imaging
Theranostic radiopharmaceutical
Redox potential

ABSTRACT

An important contributing factor to the growth of aggressive and treatment-resistant tumors is tumor hypoxia. In this investigation, we created a unique tracer, ^{64}Cu-biacetyl-bis(4-methyl-3-semicarbazone) Complex (^{64}Cu-[APSC]$_2$), for hypoxia imaging. Numerous spectral and electrochemical analyses were used to characterize the synthesized ligand and its metal complex. The coordination of the metal in the metal complex was also supported by DFT (B3LYP model) calculations. The radiochemical yields and purities of ^{64}Cu-[APSC]$_2$ were found to be quantitative, as determined by TLC and HPLC analyses.

Stability studies in human plasma demonstrated that ^{64}Cu-[APSC]$_2$ remained steady for at least four hours while being incubated at 37 °C. MDA-MB-231 cell-line xenografts were placed in nude mice for biodistribution research. The results revealed significant accumulation of the tracer in tumors after 2 h post-injection, which correlated with the redox potential and reactive oxygen species. These findings suggest that ^{64}Cu-[APSC]$_2$ shows promising evidence as a theranostic radiopharmaceutical for hypoxic tumors.

1. Introduction

Bifunctional chelators derived from bis-thiosemicarbazones have shown promise in radiopharmaceutical chemistry, particularly in hypoxia imaging (Arano et al., 1987; McPherson et al., 1990). Low tissue oxygenation, or tumor hypoxia, is a harmful state linked to radiotherapy resistance, malignant progression, and a dismal prognosis. Positron emission tomography (PET) employing the tracer [^{64}Cu] [Cu-diacetyl-bis(N(4)-methyl thio semi carbazone)] is one technique for identifying tumor hypoxia. ^{64}Cu-ATSM (Cowley et al., 2007; Bonnitcha et al., 2008).

Fujibayashi and co-workers, (Fujibayashi et al., 1997; Dearling et al., 2002) have created ^{64}Cu-ATSM, which seems to be more suitable for imaging tissues that are hypoxic. When Cu-ATSM interacts with thiol groups or redox-active proteins with NADH acting as an enzymatic cofactor, it displays a distinct behavior. This results in variations in 64Cu accumulation among different cell lines, indicating disparate uptake kinetics, maximum accumulation, and oxygen-dependent responses (Fujibayashi et al., 1997; Dearling and Blower, 1998; Holland et al., 2007). Cu-ATSM demonstrates rapid uptake and a higher hypoxic/normoxic tissue activity ratio, which can be attributed to its enhanced membrane permeability and faster blood clearance compared to other tracers like FMISO (Liu et al., 2020). Studies have illustrated that complexes with lower $E_{1/2}$ values, indicative of reduced reducibility, exhibit hypoxia selectivity, unlike easily reducible complexes (Dearling et al., 2002; Maurer et al., 2002).

However, ^{64}Cu-ATSM, like FMISO, is decreased and retained in tissue that is hypoxic or normoxic. Its slow blood clearance and low target-to-background ratio have also restricted its application in clinical settings. It has been demonstrated that ^{64}Cu-ATSM preferentially accumulates in hypoxic cells, rapidly separates from the blood, and quickly washes out of normoxic cells. (Lewis et al., 1999; Dehdashti et al., 2003).

To address these limitations, we have been investigating methods to control redox potential and lipophilicity independently by substituting alkyl groups at the diimine backbone and terminal nitrogen atoms, respectively. As a result, complexes with and without selectivity for hypoxic cells have been developed.

In this article presents a novel asymmetric compound containing a pyridine group as a potential improvement over the parent Cu-ATSM in terms of hypoxic selectivity. The compound has been radiolabeled with ^{64}Cu, and its physicochemical properties, we evaluate its cellular uptake

Peer review under responsibility of King Saud University
* Corresponding author.
E-mail address: nhokbany@ksu.edu.sa (N. Alhokbany).

https://doi.org/10.1016/j.jksus.2024.103398
Received 10 June 2024; Received in revised form 15 August 2024; Accepted 16 August 2024
Available online 17 August 2024

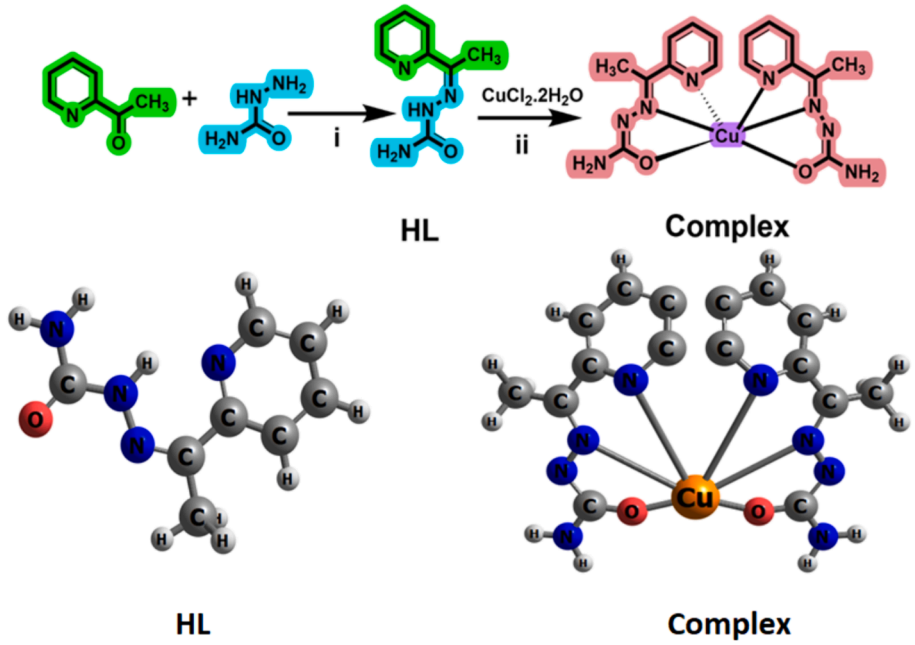

Scheme 1. Synthesis of acetyl-bis(4-methyl-3-semicarbazone) (APSC) ligand (HL) and Cu-biacetyl-bis(4-methyl-3-semicarbazone) (Cu-[APSC]$_2$) complex (CuL).

in MDA-MB-231 cells under hypoxic conditions and further investigate its performance through acute biodistribution studies.

2. Experimental: Materials and methods

The detailed materials and methods used in this study are provided in the supplementary information (SF).

2.1. Synthesis of (APSC)H: HL ligand

The compound acetyl-bis(4-methyl-3-semicarbazone) (APSC)H: HL was synthesized according to a previously reported method (Al-Hokbany et al., 2014). The detailed procedure is as follows: in the presence of sodium acetate (1.36 g, 1.0 mmol), an aqueous solution of semicarbazide hydrochloride (1.11 g, 1.0 mmol) was added to an aqueous solution of 2-acetyl pyridine (1.20 g, 1.0 mmol). For two hours, the reaction mixture was vigorously stirred. After filtering and an ether wash, the crystalline white result produced a 96 % yield. M.p 188–192 °C. Elemental analysis showed the following composition: C: 54.0 % (calculated: 53.9 %), H: 5.8 % (calculated: 5.7 %), and N: 31.2 % (calculated: 31.4 %).FTIR (υ_{max}/cm^{-1}): (NH, 3473), (NH$_2$, 3375), (CH$_3$, 2280), (C=O$_{as}$, 1686), (C=O$_{sy}$, 1579), (C=N, 1443), (C–O, 1104), and various peaks for heterocyclic bases. NMR spectroscopy indicated peaks at 3.39 ppm (3H, CH$_3$), 7.3 ppm (2H, NH$_2$), 7.3 ppm (1H, CH=C), 7.7 ppm (1H, CH=C), 8.3 ppm (1H, CH–C), 8.5 ppm (1H, CH–N), and 9.5 ppm (1H, NH). Mass spectroscopy showed a peak at *m/z* 179 ([M]$^+$).

2.2. Synthesis of Cu-biacetyl-bis(4-methyl-3-semicarbazone) complex: Cu (APSC)$_2$

Hot ethanol (EtOH, 10 mL) was used to dissolve the ligand APSC (0.019 g, 0.106 mmol), and $CuCl_2$ was added dropwise to the EtOH solution (1 mL, 0.05 mmol). For three hours, the reaction mixture was refluxed while being constantly stirred. The precipitate was filtered and then cleaned with ether once it had cooled to room temperature. Yield: 89 %. decomposed at 220 °C. The empirical formula of the complex was determined as $[C_{16}H_{20}N_8O_2]Cu$. Elemental analysis (calculated): C: 49.79 (48.63 %), H: 4.89 (4.85 %),N: 27.57 (28.36 %). FTIR (υ_{max}/cm^{-1}): (OH, 3387); (NH$_2$, 3268); (CH$_3$, 2320); (C=0$_{as}$, 1686); (C=O$_{sy}$, 1579); (C=N, 1449); (C-O, 1103); (Cu–N, 564); (Cu–O, 482); (heterocyclic bases, 771, 626, 561, 448).UV/Vis spectroscopy in DMSO (wavelength in nm, molar absorptivity in mol^{-1}dm^{3}cm^{-1}): λ_{max} = 230 (1500), 290 (800), 455 (1300).Molar conductivity (1x10^{-3} mol/L in DMF): 0.54 mS.cm^{-1}.HPLC retention time: 7.5 min.

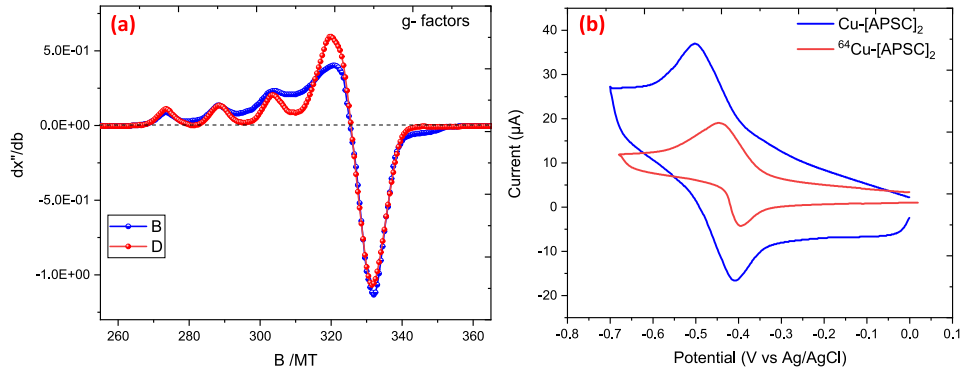

Fig. 1. (a) displays the X-band EPR spectrum of the Cu-biacetyl-bis(4-methyl-3-semicarbazone) complex in DMF. (b) cyclic voltametric chart of Cu-Complex.

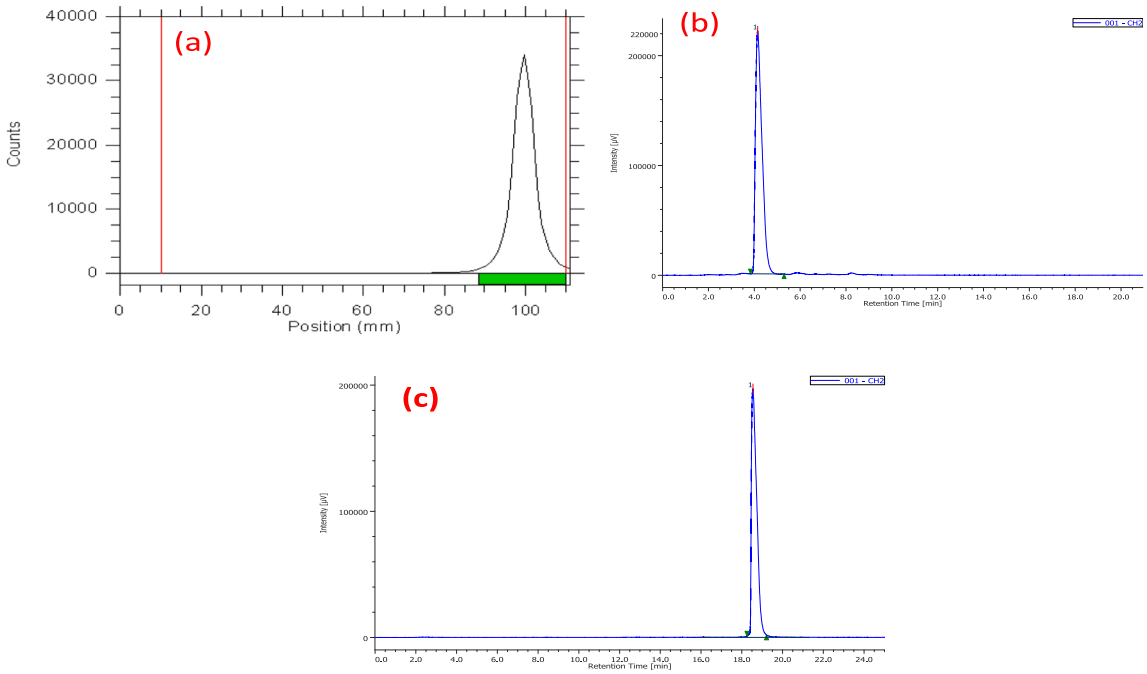

Fig. 2. (a) TLC chromatogram of (^{64}Cu-[APSC]$_2$), HPLC chromatograms of (b) $^{64}CuCl_2$ and (c) (^{64}Cu-[APSC]$_2$) complex.

2.3. Synthesis of ^{64}Cu-biacetyl-bis(4-methyl-3-semicarbazone) complex: ^{64}Cu(APSC)$_2$

$^{64}CuCl_2$ was produced via reported methods explained in the supporting information (AlHokbany et al., 2022). To a sealed vial containing 370 MBq of $^{64}CuCl_2$; 200 µg of APSC was added along with 1.2 mL of sodium acetate buffer (5 M, pH~4.6). The reaction, which was the same as the one described in support information scheme, was conducted for 30 min at 95 °C. Following the reaction, the mixtures were run through a C18 Sep-Pak cartridge after being diluted with 3 mL of water (H_2O). After the eluted solution was dried, the dried mixture was extracted from the cartridge using ethanol (EtOH). This produced about 314.5 MBq of activity in 1 mL of ethanol. After that, the ethanol was evaporated and the residue was mixed back together with regular saline. Next, a 0.22 µm pore membrane filter was used to filter the reconstituted solution so that it could be used in both in vitro and in vivo experiments.

3. Results and discussion

The Cu-[APSC]$_2$ complex was successfully obtained by reacting APSC with $CuCl_2$, resulting in a high yield, as illustrated in Scheme 1. The supporting figures SF-1 to SF-5 provide the detailed spectroscopic data for the synthesized compounds.

The EPR spectra provide valuable information about the electronic and geometric structure of the Cu(II) complex, as well as the nature of its ligand environment. In Fig. 1(a), the g-values are reported as: g_1 = 2.0650, g_2 = 2.0762, g_3 = 2.285. The magnetic hyperfine coupling constant, Az, is measured as 169 x 10^{-4} cm^{-1} for the I=3/2 nucleus of (^{63}Cu/^{65}Cu). Two signals have been identified in the EPR spectrum: one at g = 2 and the other at the half-field. These signals are thought to originate from the ΔMs=±1 and ΔMs=±2 transitions, respectively. These transitions show that a binuclear complex is forming. The unpaired electron on copper appears to have dx2-y2 character, according to the trend in the g-values ($g_\parallel > g^\perp > 2$), suggesting a square planar structure for the complex (Dearling et al., 2002; West et al., 1994).

The modulation of cellular retention and hypoxia selectivity in the copper complex is largely dependent on the reduction potential of the Cu (II) component, as demonstrated in Fig. 1(b). Hypoxia selectivity is demonstrated by complexes with an $E_{1/2}$ value less than −0.50 V, whereas easily reducible complexes lack this selectivity. This class of complexes' redox capacity plays a significant role in determining how well they retain cells and how selectively they react to hypoxia. Using $Ag/AgNO_3$ as the reference electrode, cyclic voltammetry was used to examine the redox potentials of the [Cu^{II}L]0/[Cu^{I}L]- couples in dry DMSO at 20 °C in order to better understand the biological behavior of these new complexes. (Dearling and Blower, 1998). The $E_{1/2}$ value of −0.48 V for the Cu-[APSC]$_2$ complex is in close agreement with the value of −0.54 V reported for Cu-ATSM (Dearling et al., 2002). The characteristics of the complex are changed when the methyl group at the BTSC chelator's N-terminus is swapped out for a pyridine ring, more especially, its nitrogen atom (Palma et al., 2017). Furthermore, because the oxygen atom withdraws electrons, changing sulfur to oxygen as the donor atom alters the properties of the complex. Because of this interaction, the metal's electronic density is increased, which raises the potential for reduction of −0.48 V for Cu-[APSC]$_2$.

The following is a summary of the connections between structure, lipophilicity, redox potential, and hypoxia selectivity: Firstly, the redox potential has a significant influence on hypoxia selectivity. Reduced reduction potential complexes (<-0.50 V) show improved hypoxia selectivity. Secondly, lipophilicity is not a sign of hypoxia selectivity, even though it is required for cell membrane penetration. (Castle et al., 2003; McQuade et al., 2005). The complexes generally have log P values greater than zero. The log P value for the ^{64}Cu-[APSC]$_2$ complex was found to be 1.34 ± 0.05, indicating it is relatively more hydrophilic compared to ^{64}Cu-ATSM (log P=1.85 ± 0.05) (Dearling and Blower, 1998; Green et al., 1988).

The TLC showed that the Rf value for $^{64}CuCl_2$ was 0.0, while the Rf value for the ^{64}Cu-[APSC]$_2$ complex was 0.9 (Fig. 2a). This significant difference in Rf values indicates a substantial change in the polarity and lipophilicity of the ^{64}Cu-[APSC]$_2$ complex compared to the precursor $^{64}CuCl_2$.

Furthermore, the HPLC analysis revealed distinct differences in the retention times between $^{64}CuCl_2$ and the ^{64}Cu-[APSC]$_2$ complex (Fig. 2b, c). These chromatographic results demonstrate the successful formation of the ^{64}Cu-[APSC]$_2$ complex and its distinct separation from the starting material, $^{64}CuCl_2$.

The ^{64}Cu-[APSC]$_2$ complex exhibited good stability in plasma. Proteolytic degradation studies showed that the complex remained over 95

Table 1
Biodistribution of (^{64}Cu-[APSC]$_2$) in tumor bearing nude mice.

organ	1 h	2 h	6 h
Blood	7.75 ± 0.78	4.35 ± 0.03	1.70 ± 0.13
Liver	5.09 ± 0.09	4.01 ± 0.13	1.59 ± 0.10
Lung	7.42 ± 0.17	2.84 ± 0.18	1.83 ± 0.17
Kidney	6.02 ± 0.05	3.66 ± 0.23	2.67 ± 0.03
Intestine	5.03 ± 0.04	4.71 ± 0.06	3.17 ± 0.79
Heart	6.15 ± 0.11	2.27 ± 0.38	1.0 ± 0.09
Muscle	2.24 ± 0.59	1.56 ± 0.16	0.42 ± 0.25
Spleen	5.26 ± 0.24	2.5 ± 0.18	2.25 ± 0.11
Tumor	2.80 ± 0.14	4.74 ± 0.19	2.51 ± 0.14
Tumor/muscle	1.25	3.03	5.97

For n = 3, the values are the average of the percent injected dose/gram ± SD. A radiotracer called ^{64}Cu-[APSC]2 was injected into the animals.

% intact during incubation at 37 °C and maintained this stability for up to 4 h.

The ^{64}Cu-[APSC]$_2$ complex's biodistribution was assessed in naked mice that were given xenografts of the human MDA-MB-231 cell line (Table 1). High blood uptake of the complex was observed one hour after injection. (7.75 % ID/g), which gradually decreased to 4.35 % ID/g by 2 h. This contrasts with the more lipophilic ^{64}Cu-ATSM, which is rapidly and efficiently cleared from the blood (3.65 % ID/g at 1 min, and 2.22 % ID/g over 4 h) (Bonnitcha et al., 2008; Lewis et al., 1999). The liver uptake of ^{64}Cu-[APSC]$_2$ was 5 % ID/g at 1 h, significantly lower than the 20.84 % ID/g observed for ^{64}Cu-ATSM at the same time point (Lewis et al., 1999; McQuade et al., 2005). Other major organs, including the lungs, heart, spleen, and kidneys, also showed high initial uptake, but the radioactivity began to clear by 2 h post-injection. The tumor uptake of ^{64}Cu-[APSC]$_2$ reached an optimal peak of 4.76 ± 0.19 % ID/g at 2 h post-injection, comparable to to the highest tumor uptake recorded for ^{64}Cu-ATSM (4.78 ± 1.00 % ID at 10 min) (Lewis et al., 1999; McQuade et al., 2005; Bonnitcha et al., 2008). At two hours, the tumor-to-muscle ratio was 3.1, indicating that the radiotracer had accumulated favorably in the tumor tissue.

4. Computational results

Molecular modeling using density functional theory (DFT) at the B3LYP level was conducted to examine the structures of the ligand and the Cu-[APSC]$_2$ complex. The optimized structures, shown in Scheme 1, indicate that the Cu(II) center has a hexacoordinate bonding mode in the complex. The DFT-computed bond lengths and angles are reported in Supporting Figure SF-6.

In the complex, the Cu(II) center is coordinated to the oxygen atoms of the two ligand (L1 and L2) molecules. The bond lengths are 1.898 Å for both the Cu–O(40) and Cu–O(26) bonds. The bond angles in the complex show some variation: For the L2 ligand, the C(24)-O(26)-Cu (41) angle is 158.5°. For the L1 ligand, the C(36)-O(40)-Cu(41) angle is 158.7°. The O(26)-Cu(41)-O(40) angle between the two ligands is 149.5°. The bond angles in the complex range from 158.7° to 90°, and the bond lengths range from 1.898 Å to 1.006 Å. The longest bond length is observed for the O(26)-Cu(41) bond.

In the free ligand, the bond length range is 1.863 Å to 1.006 Å, with the maximum value observed for the N(6)-C(18) bond. The bond angle range is 139.3° to 101.5°, with the maximum value observed for the C (1)-N(6)-C(18) angle. The DFT-calculated geometric parameters for both the ligand and the complex are in good agreement, providing a solid starting point for further property calculations and understanding the complex's structural characteristics.

Table 3
The chemical reactivity **parameters** (in eV) calculated at the B3LYP/6-31G(d, p) level of theory.

Molecules	IP	EA	η	ω	χ	μ	σ
HL	5.846	1.541	2.152	3.169	3.693	−3.693	0.232
Complex	4.694	1.949	1.372	4.019	3.321	−3.321	0.364

Frontier molecular orbitals have two crucial quantum chemical properties: the lowest unoccupied molecular orbital (LUMO) and the highest occupied molecular orbital (HOMO). These properties can be used to assess a compound's reactivity, where the HOMO and LUMO represent the electron donor and acceptor behavior, respectively. The energy difference between HOMO and LUMO, known as the energy gap (ΔE), is a crucial factor in predicting the molecule's electrical transport properties. A smaller ΔE value indicates a more reactive system. The data in Table 2 shows that the free ligand (HL) has the largest energy gap of 4.305 eV, while the complex species have a smaller energy gap of 2.745 eV, suggesting the latter are more stable.

Using the equations {1–7}, the values of electronegativity (χ), chemical potential (μ), global hardness (η), and global softness (σ) were determined (Humphrey et al., 1996), and these values were reported in Table 3 and Fig. 3. Based on these characteristics, the HL ligand and the complex have the best electron-accepting capacity, the best stabilization energy, and the lowest chemical hardness, making them potentially suitable for use in the medical field.

$$IP = -E_{HOMO} \tag{1}$$

$$EA = -E_{LUMO} \tag{2}$$

$$\sigma = \frac{1}{2\eta} \tag{3}$$

$$\eta = \frac{[IP - EA]}{2} = -\frac{[E_{LUMO} - E_{HOMO}]}{2} \tag{4}$$

$$\omega = \frac{(IP + EA)^2}{4(IP - EA)} \tag{5}$$

$$X = \frac{[IP + EA]}{2} = -\frac{[E_{LUMO} + E_{HOMO}]}{2} \tag{6}$$

$$\mu = \frac{E_{HOMO} + E_{LUMO}}{2} \tag{7}$$

5. Conclusion

The synthesis of ^{64}Cu-[APSC]$_2$ resulted in excellent radiochemical yield and purity within a short time frame of less than 30 min. At two hours post-injection (p.i.), biodistribution studies using human MDAMB-231 cell line xenografts in a model of naked mice demonstrated a significant accumulation of ^{64}Cu-[APSC]$_2$ in tumor tissue, indicating substantial tumor uptake. Furthermore, the pharmacokinetic profile of ^{64}Cu-[APSC]$_2$ was favorable compared to previously investigated radiotracers of its kind.

The theoretical stability of the compound was determined using advanced quantum chemistry simulations, including DFT and TD-DFT

Table 2
The HOMO-LUMO, band gap (eV) calculated.

Molecules	HOMO (eV)	LUMO (eV)	Energy gap (eV)	HOMO-1	LUMO+1	Energy gap (eV)
HL	−5.846	−1.541	4.305	−6.668	−0.945	5.724
Complex	−4.694	−1.949	2.745	−5.405	−1.432	3.973

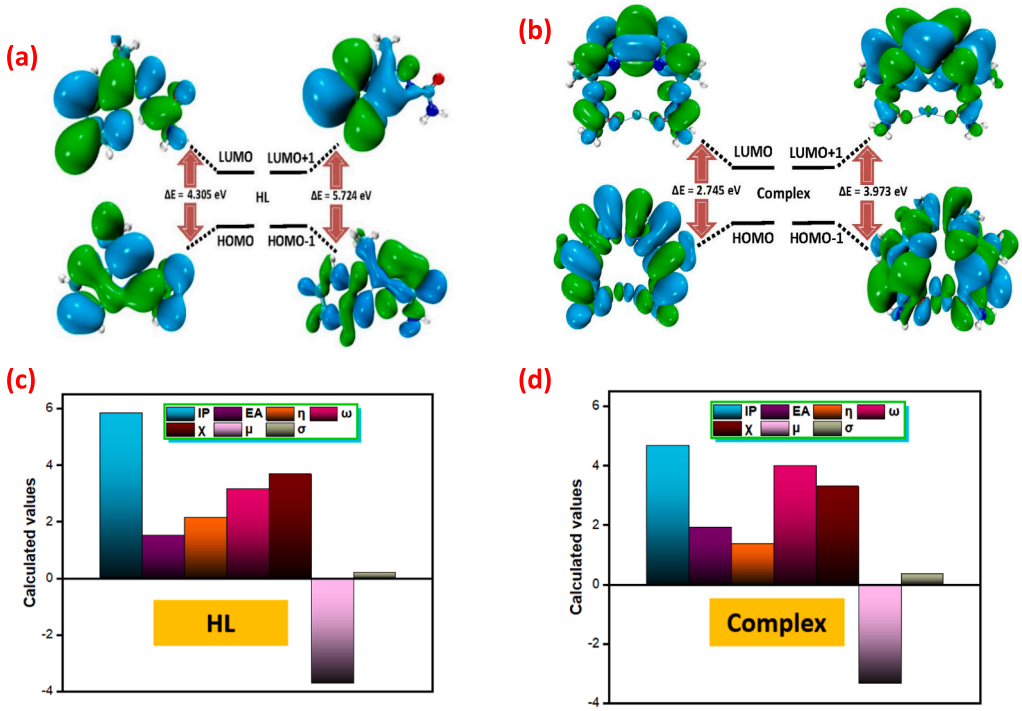

Fig. 3. The Contour plots representing HOMO and LUMOs of (a,c) HL and (b,d) complex.

methods. The complex under investigation exhibits promising anti-cancer activity, according to analyses of its frontier molecular orbitals (FMO), natural bond orbitals (NBO), geometric parameters, electron localization function (ELF), non-covalent interactions (NCI), localized orbital locator (LOL), molecular electrostatic potential (MEP), and Mullikan charge. This implies possible uses in the creation of innovative medications. Significantly, it was discovered that the low end of the range's redox potential was necessary for hypoxia selectivity, a desirable quality for the compound's use in tumor detection and staging.

Overall, the findings from this study suggest that the ^{64}Cu-[APSC]$_2$ radiotracer holds promise as a PET probe for the detection and staging of hypoxic tumors. However, further evaluation and investigation are necessary to fully validate its potential clinical utility.

CRediT authorship contribution statement

N. Alhokbany: Writing – review & editing, Project administration, Data curation, Conceptualization. **I. Aljammaz:** ^{64}Copper production. **B. Alotaibi:** Labeling compound, Data curation. **Y. AlMalki:** Biodistribution studies. **S. Almasaari:** Technical analysis.

Declaration of competing interest

The authors declare that they have no known competing financial interests or personal relationships that could have appeared to influence the work reported in this paper.

Acknowledgements

This project was supported by King Abdulaziz City for Science and Technology (KACST), Saudi Arabia-National Plan Project No. (11-MED1761-02).

Appendix A. Supplementary material

Supplementary data to this article can be found online at https://doi.org/10.1016/j.jksus.2024.103398.

References

AlHokbany, N., AlJammaz, I., AlOtaibi, B., AlMalki, Y., AlJammaz, B., Okarvi, S.M., 2022. Development of new copper-64 labeled rhodamine: A potential PET myocardial perfusion imaging agent. EJNMMI Radiopharm. Chem. 7 (1), 19.

N. S. Al-Hokbany, Basim Alotaibi, Suad Bin Amer, Subhani M. Okarvi, and Ibrahim Al-Jammaz., Synthesis and *In Vitro* and *In Vivo* Evaluation of a New 68Ga-Semicarbazone Complex: Potential PET Radiopharmaceutical for Tumor Imaging., Journal of Chemistry., 2014, Article ID 616459, 6 pages DOI: 10.1155/2014/616459.

Arano, Y., Yokoyama, A., Furukawa, T., Horiuchi, K., Yahata, T., Saji, H., Sakahara, H., Nakashima, T., Koizumi, M., Endo, K., 1987. Technetium-99m-labeled monoclonal antibody with preserved immunoreactivity and high in vivo stability. J. Nucl. Med. 28 (6), 1027–1033.

Becke, A.D., 1992. Density-functional thermochemistry. I. The effect of the exchange-only gradient correction. J. Chem. Phys. 96, 2155–2160. https://doi.org/10.1063/1.462066.

P.D. Bonnitcha, A.L. Va¯vere, J.S. Lewis, J.R. Dilworth, In vitro and in vivo evaluation of bifunctional bisthiosemicarbazone 64Cu-complexes for the positron emission tomography imaging of hypoxia, Journal of medicinal chemistry 51(10) (2008) 2985-2991.

Castle, T.C., Maurer, R.I., Sowrey, F.E., Went, M.J., Reynolds, C.A., McInnes, E.J.L., Blower, P.J., 2003. Hypoxia-targeting copper bis(selenosemicarbazone) complexes: Comparison with their sulfur analogues. J. Am. Chem. Soc. 125 (33), 10040–10049.

Cowley, A.R., Dilworth, J.R., Donnelly, P.S., Heslop, J.M., Ratcliffe, S.J., 2007. Bifunctional chelators for copper radiopharmaceuticals: The synthesis of [Cu(ATSM)–amino acid] and [Cu(ATSM)–octreotide] conjugates. Dalton Trans. (2), 209–217.

Dearling, J.L., Blower, P.J., 1998. Redox-active metal complexes for imaging hypoxic tissues: structure–activity relationships in copper (II) bis (thiosemicarbazone) complexes. Chem. Commun. (22), 2531–2532.

Dearling, J.L., Lewis, J.S., Mullen, G.E., Welch, M.J., Blower, P.J., 2002. Copper bis (thiosemicarbazone) complexes as hypoxia imaging agents: Structure-activity relationships. J. Biol. Inorg. Chem. 7 (3), 249–259.

Dehdashti, F., Perry, W., Grigsby, M.A., Mintun, J.S.L., Siegel, B.A., Welch, M.J., 2003 Apr 1. Assessing tumor hypoxia in cervical cancer by positron emission tomography with 60Cu-ATSM: Relationship to therapeutic response-a preliminary report. Int. J. Radiat. Oncol. Biol. Phys. 55 (5), 1233–1238. https://doi.org/10.1016/s0360-3016(02)04477-2.

R. Dennington, T. Keith, J. Millam ., GaussView, Version 5.0.8.: Semichem Inc., Shawnee Mission KS; 2009.

M.e. Frisch, G. Trucks, H.B. Schlegel, G. Scuseria, M. Robb, J. Cheeseman, G. Scalmani, V. Barone, G. Petersson, H. Nakatsuji, Gaussian 16, Gaussian, Inc. Wallingford, CT, 2016.

Fujibayashi, Y., Taniuchi, H., Yonekura, Y., Ohtani, H., 1997. Copper-62-ATSM: a new hypoxia imaging agent with high membrane permeability and low redox potential. J. Nucl. Med. 38 (7), 1155.

Green, M.A., Klippenstein, D.L., Tennison, J.R., 1988. Copper (II) bis (thiosemicarbazone) complexes as potential tracers for evaluation of cerebral and myocardial blood flow with PET. J. Nucl. Med. 29 (9), 1549–1557.
Holland, J.P., Aigbirhio, F.I., Betts, H.M., Bonnitcha, P.D., Burke, P., Christlieb, M., Churchill, G.C., Cowley, A.R., Dilworth, J.R., Donnelly, P.S., 2007. Functionalized bis (thiosemicarbazonato) complexes of zinc and copper: Synthetic platforms toward site-specific radiopharmaceuticals. Inorg. Chem. 46 (2), 465–485.
Humphrey, W., Dalke, A., Schulten, K., 1996. VMD: visual molecular dynamics. J. Mol. Graph. 14 (1), 33–38. https://doi.org/10.1016/0263-7855(96)00018-5.
Jammaz, I.A., Al-Otaibi, B., Al-Hokbani, N., Okarvi, S.M., 2019. Synthesis of novel gallium-68 labeled rhodamine: A potential PET myocardial perfusion agent. Appl. Radiat. Isot. 144, 29–33.
Lewis, J.S., McCarthy, D.W., McCarthy, T.J., Fujibayashi, Y., Welch, M.J., 1999. Evaluation of 64Cu-ATSM in vitro and in vivo in a hypoxie tumor model. J. Nucl. med 40 (1), 177–183.
Lewis, J.S., McCarthy, D.W., McCarthy, T.J., Fujibayashi, Y., Welch, M.J., 1999. Evaluation of 64Cu-ATSM in vitro and in vivo in a hypoxic tumor model. J. Nucl. Med. 40 (1), 177–183.
Liu, T., Karlsen, M., Karlberg, A.M., Redalen, K.R., 2020. Hypoxia imaging and theranostic potential of [64Cu][Cu (ATSM)] and ionic Cu (II) salts: a review of current evidence and discussion of the retention mechanisms. EJNMMI Res. 10 (1), 1–14.
T. Lu, F. Chen., Multiwfn: A multifunctional wavefunction analyzer., 2011., DOI: 10.1002/jcc.22885.
Maurer, R.I., Blower, P.J., Dilworth, J.R., Reynolds, C.A., Zheng, Y., Mullen, G.E.D., 2002. Studies on the mechanism of hypoxic selectivity in copper bis (Thiosemicarbazone) radiopharmaceuticals. J. Med. Chem. 45 (7), 1420–1431.
R.A. May, K.J. Stevenson, Software review of Origin 8, ACS Publications, 2009.
McPherson, D., Umbricht, G., Knapp Jr, F., 1990. Radiolabeling of proteins with radioisotopes of copper using p-carboxyalkylphenylglyoxal bis-(4N-methylthiosemicarbazone)(TSC) bifunctional chelates. J. Label. Compd. Radiopharm. 28 (8), 877–899.
McQuade, P., Martin, K.E., Castle, T.C., Went, M.J., Blower, P.J., Welch, M.J., Lewis, J.S., 2005. Investigation into 64Cu-labeled Bis (selenosemicarbazone) and bis (thiosemicarbazone) complexes as hypoxia imaging agents. Nucl. Med. Biol. 32 (2), 147–156.
O'Boyle, N.M., Tenderholt, A.L., Langner, K.M., 2008. Cclib: A library for package-independent computational chemistry algorithms. J. Comput. Chem. 29, 839–845. https://doi.org/10.1002/jcc.20823.
Palma, E., Mendes, F., Morais, G.R., Rodrigues, I., Santos, I.C., Campello, M.P.C., Raposinho, P., Correia, I., Gama, S., Belo, D., 2017. Biophysical characterization and antineoplastic activity of new bis (thiosemicarbazonato) Cu (II) complexes. J. Inorg. Biochem. 167, 68–79.
West, D.X., Gebremedhin, H., Romack, T.J., Liberta, A.E., 1994. Spectral and biological studies of copper(II) complexes of 2-acetyl-pyridine thiosemicarbazones with bulky 4N-substituents. Transit. Met. Chem. 19 (4), 426–431.
Zhurko, G. and Zhurko, D. (2015) Chemcraft Graphical Program for Visualization of Computed Results.., http://www.chemcraftprog.com/.